# Polymer Electrolyte Glue: A Universal Interfacial Modification Strategy for All-Solid-State Li Batteries

*Derui Dong,[1,†] Bin Zhou,[1,†] Yufei Sun,[1] Hui Zhang,[2] Guiming Zhong,[3] Qingyu Dong,[4] Fang Fu,[1] Hao Qian,[1] Zhiyong Lin,[1] Derong Lu,[5] Yanbin Shen,[4] Jihuai Wu,[1] Liwei Chen,[4,6]* and Hongwei Chen[1]*

[1] College of Materials Science and Engineering, Huaqiao University, Xiamen 361021, China

[2] State Key Laboratory for Mechanical Behavior of Materials, School of Materials Science and Engineering, Xi'an Jiaotong University, Xi'an 710049, China

[3] Xiamen Inst Rare Earth Mat, Chinese Academy of Sciences, Xiamen 361021, China

[4] i-LAB, Suzhou Institute of Nano-Tech and Nano-Bionics (SINANO), Chinese Academy of Sciences, Suzhou 215123, China

[5] School of Chemical and Biomedical Engineering, Nanyang Technological University, 70 Nanyang Drive, 637457, Singapore

[6] In-situ Center for Physical Sciences, School of Chemistry and Chemical Engineering, Shanghai Jiao Tong University, Shanghai 200240, China

† These authors contributed equally to this work.

*Correspondence and requests for materials should be addressed to L.W.C. (lwchen2008@sinano.ac.cn) and H.W.C. (email: hwchen@hqu.edu.cn).

**ABSTRACT:** In recent years solid $Li^+$ conductors with competitive ionic conductivity to those of liquid electrolytes have been reported. However, the incorporation of highly conductive solid electrolytes into the lithium-ion batteries is still very challenging mainly due to the high resistance existing at the solid-solid interfaces throughout the battery structure. Here, we demonstrated a universal interfacial modification strategy through coating a curable polymer-based glue electrolyte between the electrolyte and electrodes, aiming to address the

poor solid-solid contact and thus decrease high interfacial resistance. The liquid glue exhibits both great wettability as well as chemical/electrochemical stability to most of the electrodes, and it can be easily solidified into a polymer electrolyte layer through a "post-curing" treatment. As a result, symmetric Li batteries with the glue modification exhibit much smaller impedance and enhanced stability upon plating/stripping cycles compared to the batteries without glue modification. The all-solid-state Li-S batteries with glue modification show significantly enhanced performances. The strategy of developing glue electrolytes to improve the electrode-electrolyte interface contact provides an alternative option for improving many other solid-state batteries.

**KEYWORDS:** polymer electrolyte, glue, interface, solid-state battery

Conventional lithium-ion batteries (LIBs) pose both flammable and explosion risks because of the use of liquid organic electrolytes.[1] All-solid-state LIBs are thus increasingly receiving attention in recent years, because the solid-state chemistry not only effectively improve the safety of LIBs by replacing the flammable organic electrolytes with solid-state electrolytes but also increase the possibility to realize a lithium metal anode (with the highest specific capacity (3861 mAh/g) and lowest redox potential (-3.04 V vs SHE)), which will facilitate the development of next-generation LIBs with a higher energy density and better safety.[2-6] Most of the reported work on all-solid-state LIBs has been focusing on increasing the bulk conductivity of solid-state electrolytes and electrodes, although the interface issues within the solid-state LIBs are also challenging obstacles, including but not limited to interfacial contact, space charge region, or the formation of interphase.[7-10] Although a comprehensive approach to solve all the interfacial issues cannot be easily obtained because of the large variety of LIB systems involved, the importance of constructing a great solid-solid interfacial contact for the all-solid-state LIBs has been widely recognized.[10, 11] This

is determined by the rigid nature of the current widespread inorganic cathode or anode materials, as well as the inorganic solid electrolytes used for LIBs. Most of these inorganics are deformation resistant, resulting in large interfacial resistance between the solid electrolytes and electrode films in the solid-state cell due to poor solid-solid contact.

For a complete discharge-charge process of all-solid-state LIBs, the $Li^+$ migrate back and forth between the cathode and anode films. So an ideal interfacial modification strategy should be able to resolve the contact issues both for the cathode-electrolyte and anode-electrolyte interface. Several effective approaches, for example by adding $Al_2O_3$ or amorphous Si functional layer at anode-electrolyte interfaces, have been reported, while the cathode-electrolyte interface issues attracted less attention so far.[12, 13] Encouragingly, a few modification approaches for cathode-electrolyte interface were reported recently using, for example, soft polymers or small-molecule organics as buffer layers for the rigid solid inorganic electrolytes, even though the poor thermal stability of small-molecule organics may limit high-temperature operation for the batteries.[14, 15] Besides, at present, most of the effective interfacial modification approaches are developed based on the relative time-consuming physical deposition methods, such as atomic layer deposition (ALD). Developing a simple and cost-efficient strategy applicable to both cathode/anode-electrolyte interface modifications is the key challenge for the realization of high-performance all-solid-state LIBs.

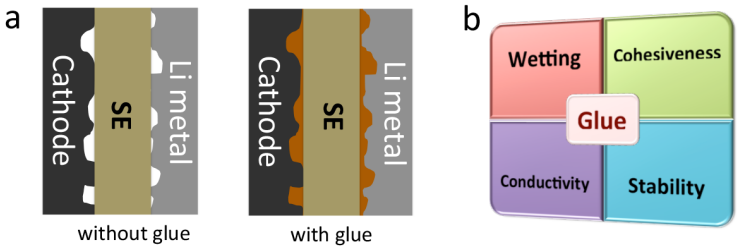


**Figure 1.** (a) Schematic diagram for all solid-state batteries with or without the electrolyte glue. (b) General properties required for good electrolyte glues.

Herein, we demonstrated a new strategy using of a polymer electrolyte "glue", i.e., a liquid at room temperature but can be solidified to form a solid electrolyte polymer with rising

temperatures, to address the electrode (including both cathode and anode)-electrolyte interfacial contact challenge (Figure 1(a)). An A+B complex strategy was employed to construct the glue. A cross-linkable precursor resin used as item A, functioning as both an adhesive binder and an ionic conductor, was dissolved in some special solvents (i.e., item B) to form a glue solution. The as-prepared glue solution was then coated on the electrode-electrolyte interface. With a continuous heat-curing process (i.e. liquid transforms into solid), the precursor resin in the glue solution was gradually polymerized into a solid polymer along with the evaporation of the solvents. This heating process was called "post-curing stage". This special "*in-situ*" curing process of the glue on the solid-solid interface provides strong cohesiveness between the electrode-electrolyte interface, which is significantly different with the common polymer modification cells where the solid polymer layer was pre-formed on the electrode or electrolyte surface before cell assembly. Therefore, the resulting glued solid-state lithium batteries exhibit significantly reduced interfacial impedance and stable cycling at room temperature.

Ideally, the electrolyte glue should meet at least four requirements (Figure 1(b)): 1) Wettability, i.e., the ability of the glue to simultaneously infiltrate the surfaces of the electrode and solid electrolyte. 2) Adhesiveness, which is the basic function of the glue after curing. The key issue is how to design/control the curing chemistry of the glue. 3) Ionic conductivity: The glue must be both a good ionic conductor and an electronic insulator. 4) Chemical/electrochemical stability: The glue should be able to maintain its electrochemical stability during cycling in a relatively large potential window without any adverse reactions with the electrode or the solid electrolyte.

In the present study, we chose a cross-linking polymer with polymerized ionic networks as item A (named as PIN, see synthesis route in Supplementary Scheme S1). The cross-linking degree of the PIN can be easily controlled by adjusting the reaction time during synthesis. In this work, a low cross-linking PIN was used as the precursor resin of the glue

(Scheme S1 (b)). It is worth noticing that the high charge density networks of PIN could provide a suitable polarization environment for the dissociation of anion-cation pairs and thus result in high ionic conductivity (Figure 2(a)).[16] To prepare the glue from this solid precursor, succinonitrile (SN) was used as the solvent (i.e., item B) to form a glue solution (the glue was named as P@S glue hereafter). The high polarity of the SN liquid enables it to dissolve the functional additives such as Li salts, and moreover, ensures a great wetting capability of the glue solution at the solid surface.[17]

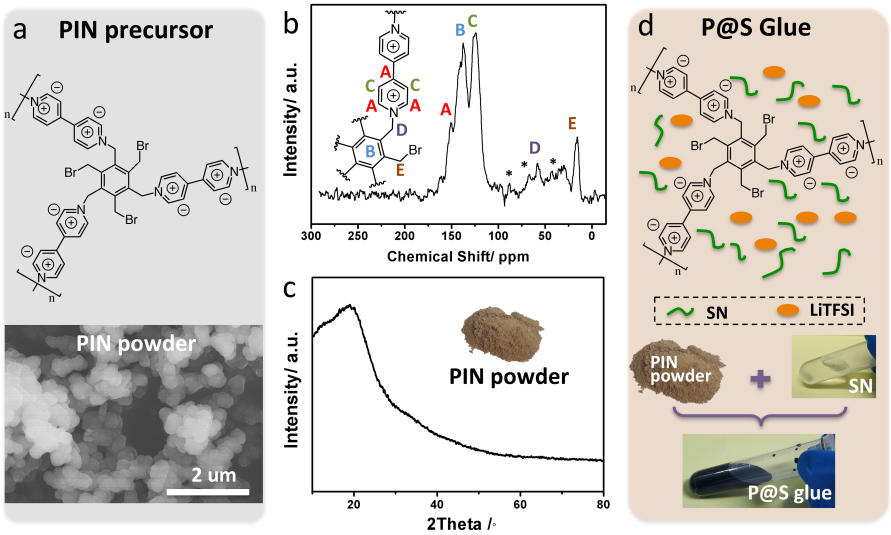


**Figure 2.** (a) Schematic molecular structure and SEM image of PIN precursor. Bottom: SEM image of PIN precursor. (b) Solid-state $^{13}C$ NMR of the PIN precursor. Asterisks indicate spinning sidebands. (c) XRD pattern of the PIN precursor. (d) Schematic diagram for the preparation of P@S glue.

The P@S glue preparation involves two steps. First, the low cross-linking PIN precursor was synthesized via the partial nucleophilic substitution between hexakis(bromomethyl)benzene and 4,4-bipyridine by controlling the reaction time, followed by an ion-exchange process to introduce TFSI anions into the framework (pre-polymerization stage, see Scheme S1((b)).[16] The as-prepared PIN powder exhibited a dispersed granular morphology with a particle size distribution in the range of hundreds of nanometers (Figure 2(a)). The molecular structure was investigated by solid-state $^{13}C$ cross-polarization magic angle spinning nuclear magnetic resonance (NMR) measurements. The signal at ~150 ppm (Figure 2(b), peak A) is attributed to the pyridinium carbon (C-2, C-4, and C-6 positions)

bearing the positive charge, and peak C (~125 ppm) is assigned to the carbons at the C-3 and C-5 positions. The B peak at ~137 ppm is ascribed to the substituted phenyl carbons. The peak D (at ~61 ppm) and peak E (at ~19 ppm) is ascribed to the result of the benzylic carbon atom close to the positive unit and the unreacted -$CH_2Br$ unit, respectively.[18] After the anion exchange, four peaks in the Fourier transform infrared (FTIR) spectra appeared (1344, 1177, 1128, and 1050 $cm^{-1}$) that could be assigned to the vibration sorption of TFSI anions (Figure S1).[19] The PIN precursor is insoluble in common organic solvents or water, possibly owing to the formation of 3D cross-linked frameworks. The absence of sharp characteristic X-ray diffraction (XRD) peak indicated that the PIN is a typical amorphous polymer (Figure 2(c)).

A SN solution was pre-prepared by dissolving a certain proportion of lithium salt (Lithium bis(trifluoromethanesulfonyl)imide, denoted as LiTFSI) into SN. The PIN precursor and the SN solution was then mixed and heated at 100 °C to form the P@S glue, which turned into a black viscous solution after more than 12 h of heating (Figure 2(d)). No precipitation was observed after high-speed centrifugation of the P@S solution, indicating that the PIN precursor was stably dispersed by the SN solvent. FTIR spectrum of the P@S glue revealed only the characteristic peaks of individual PIN and SN molecules without new peaks formed, indicating that the SN only acted as a solvent/dispersant, and no chemical reaction occurred between the PIN and SN (Figure S2). In the following section, the physicochemical properties of the P@S glue are discussed in detail.

The primary requirement for the glue is good wettability on the electrode and electrolyte surface so that a remarkable adhesive effect can be expected. Therefore, we investigated the wetting behavior of the glue on some typical LIB electrodes and electrolytes, including $LiFePO_4$, $LiCoO_2$, carbon/sulfur composite (C/S, a typical inorganic sulfur-based cathode),[20] sulfurized polyacrylonitrile (PANS, a typical organic-sulfur-based cathode),[21] graphite, Li metal and $Li_4Ti_5O_{12}$, as well as two representative solid-state electrolytes, $Li_{6.75}La_3Zr_{1.75}Ta_{0.25}O_{12}$ (LLZTO, a typical inorganic electrolyte) and polyethylene oxide (PEO,

a typical organic polymer electrolyte). All of the test materials were prepared into electrode films according to normal casting procedures (see the experimental section for details). From the contact angle measurements, we found that the contact angles of glue on the $LiFePO_4$, $LiCoO_2$, C/S composite, PANS, graphite, and $Li_4Ti_5O_{12}$ electrodes were 29.04°,13.56°, 11.45°, 6.65°, 16.88°, 22.63°, respectively (Figure 3(a) & Figure S3), suggesting the great wettability of the glue with common electrodes. Similarly, the contact angles of the glue on LLZTO and PEO electrolytes were 42.10° and 34.45°, respectively (Figure S3), also hinting the great wettability of the glue with the solid electrolytes. The wettability might be attributed to the strong polarity of the SN molecule and the appropriate surface roughness of the electrode/electrolyte surface. Notably, these results imply that the P@S glue is practicable to both of cathode-electrolyte and anode-electrolyte interfacial modification.

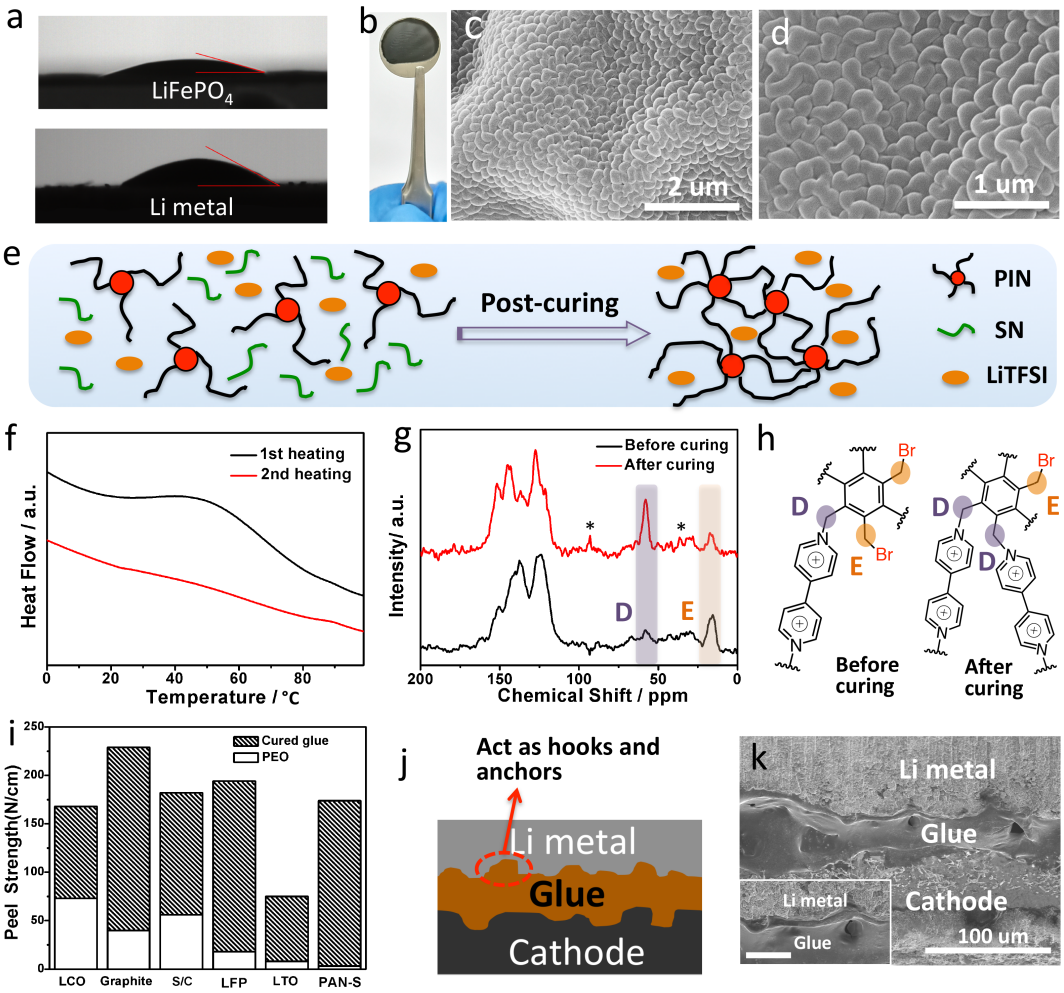

**Figure 3.** (a) Contact angle of a P@S glue droplet on the surface of $LiFePO_4$ cathode and Li metal. (b) Photograph of glue cured on stainless steel. (c)&(d) SEM images of cured PIN. (e) Schematic illustration of PIN precursor translated into high cross-linking PIN during post-curing. (f) 1st and 2nd DSC heating curves of glue. Heating at 10 °C/min under $N_2$. (g) Solid-state $^{13}C$ NMR of PIN precursor before and after curing. Asterisks indicate spinning sidebands. (h) Schematic diagram of PIN structure before and after curing. (i) Peel-off strength of glue on different electrodes and solid-state electrolytes. (j) Schematic diagram of the mechanical mosaic theory for glue adhesiveness. (k) SEM images of the cross-section of cathodelcured gluelanode cell. Scale bar in inset is 25 μm.

Another special consideration for the P@S glue design is how to realize the curing process. With the continuous heating, the volatilizable SN proceeded to evaporate, the viscosity of the glue gradually increased, and the glue eventually formed a shiny black solid (Figure 3(b)). From the SEM images in Figure 3(c-d), it can be observed that the cured PIN particles were tightly bonded to each other (see more in Figure S4 & S5). Interestingly, these particles appeared to closely bond with each other after the heat-curing process. No distinct crack or separation between the cured PIN particles was observed. Similar particle aggregation was also confirmed in the atomic force microscopy (AFM) results (Figure S6). As discussed above, the ideal PIN with high cross-linking degree was formed by the alkylation reaction of all six reactive sites of the monomer (Scheme S1(a)). By simply shortening the reaction time during the PIN precursor synthesis, the formation of high cross-linking PIN was prevented and some reactive sites of the monomer remained (Scheme S1(b)). In the subsequent heat-curing, as the concentration of the P@S glue gradually increased (SN was gradually evaporated by heating), the PIN precursor particles aggregated, and the reaction at the interfaces of the neighboring low cross-linking PIN particles continued—this process was called “post-curing”, resulting in high cross-linking PIN as well as bonded PIN particles (as illustrated schematically in Figure 3(e)).

The curing process was tracked by differential scanning calorimetry (DSC). The DSC curve of the P@S glue showed a broad endothermic peak upon heating at ~25-75 °C. However, this peak no longer appeared during the subsequent second heating (Figure 3(f)). Such thermal behavior is similar to that of common epoxy-based glues during the curing

process.[18, 22] That is, a curing reaction occurs during the heating process. Since the curing was completed at the initial heating, the endothermic peak disappeared in the following second heating process. In contrast, pure SN without PIN showed only a repeatable sharp endothermic peak at ~62 °C, corresponding to the melting of the SN molecules (Figure S7).[23] More importantly, the curing reaction was demonstrated by the $^{13}C$ NMR spectroscopy. As shown in Figure 3(g), after the curing stage, the peak E at ~19 ppm (attributed to -$CH_2$-Br in hexakis(bromomethyl)benzene monomer) declined dramatically while the peak D at ~61 ppm (attributed to -$CH_2$- carbon atom close to the positive unit) increased markedly, indicating the subsequent nucleophilic substitution of the hexakis(bromomethyl)benzene monomer during the curing.[16] The $^{1}H$ NMR results correspond to $^{13}C$ NMR results very well (Figure S8). The curing reaction was schematically illustrated in Figure 3(h). FTIR results obtained after the curing stage also proved that the curing reaction did not create a new component (Figure S9).[24] The thermogravimetric (TG) analysis suggested improved thermal stability of the PIN after curing and ~1.9 wt% residue SN was found in the final solid (Figure S10&11).

As the P@S glue exhibits great wettability and is curable, the great adhesive performance of the glue is reasonably expected. The adhesiveness of the cured glue to electrodes and electrolytes was tested and shown in Figure 3(i) (see detail in Supplementary Information). After application of the glue, a significant adhesiveness was found in all cases. All the peel-off strength (the strength when the cover tape is peeled off from the carrier tape) was estimated in the range of ~70 to 190 N $cm^{-1}$. We further selected a control polymer solution (as exemplified by PEO electrolyte) to compare its adhesive properties with the P@S glue. The PEO exhibited a significantly lower peel-off strength (generally <70 N $cm^{-1}$). The classical mechanical mosaic theory might explain the special adhesion effect of P@S glue: as the glue can easily infiltrate into the voids on the surface of the substrate and be subsequently cured, the cured PIN particles between the electrodes and electrolyte could connect the two different components by functioning as several small hooks and anchors (Figure 3(k)).[25]

Indeed, the cured PIN bonded tightly to the electrode and electrolyte layers can be clearly observed from the SEM images (Figure 3(j)). Noted that the cured layer of micron thickness shown in Figure 3(j) was only served as extreme examples for clear observation. In a real battery, the thickness of the cured glue layer can be conveniently controlled by adjusting different amounts of P@S glue, and the thickness of the adhesive layer can be controlled to below hundreds of nanometers.

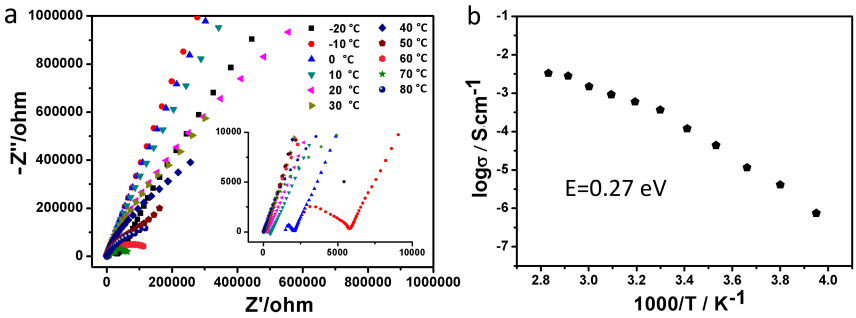


**Figure 4.** (a) EIS curves of cured P@S glue at different temperatures. (b) Ionic conductivity of cured P@S glue as a function of different temperatures.

The electrochemical properties of the cured P@S glue were thus further studied as it directly affect the performance of the all-solid-state LIBs. First and foremost, the cured glue should have a high ionic conductivity. To evaluate the ionic conductivity of the cured glue, the glue was coated and cured on the stainless steel (SS) and cells with symmetric configuration of SS|cured glue|SS were assembled in an argon-filled glovebox. The electrochemical impedance spectroscopy (EIS) data were collected and the ionic conductivity was calculated from the EIS results. The ionic conductivities slightly increased with increasing Li salt contents and reaches the maximum at 5 wt%, then drops slightly at 7 wt% (Figure S12). Thus the P@S glue containing 5 wt % Li salt was used in the following study (Figure 4(a)). The temperature dependence of the conductivities was calculated from the EIS results (Figure 4(b)). It displays the highest conductivity of $1.15\times10^{-4}$ S $cm^{-1}$ at room temperature, which is about two or three orders of magnitude higher than that of typical PEO polymer electrolyte (at room temperature).[26] As the temperature increased to 80 °C, it shows a

ionic conductivity of $6.55\times10^{-3}$ S $cm^{-1}$ which is almost comparable to that of common liquid organic electrolytes.[1] Obviously, the ionic conductivity follows a VTF relationship rather than the classical Arrhenius relationship. In general, the VTF law applies widely to disorganized matter including amorphous polymers.[27] It thus suggests that the $Li^+$ conduction in the cured P@S glue may establish by $Li^+$ diffusing in the amorphous phase of PIN, which is consistent with the amorphous structure of PIN molecules as deduced based on the XRD results. The excellent conductivity may stem from the high charge density of the PIN framework, which provides abundant, weakly coordinating sites during $Li^+$ diffusion via electrostatic interaction.[28] Meanwhile, their hierarchical and robust framework also provides a rich void for fast $Li^+$ diffusion. Another key factor of high conductivity of the cured P@S glue may be ascribed to the disappeared interface between most the PIN particles after curing stage, which in turn resulted in a continuous and facile pathway for $Li^+$ diffusion among the PIN particles. Besides the superior conductivity, the cured P@S glue also exhibited excellent electrochemical stability. No obvious decomposition of any components occurs until ~ 4.6 V versus $Li^+$/Li (Figure S13).

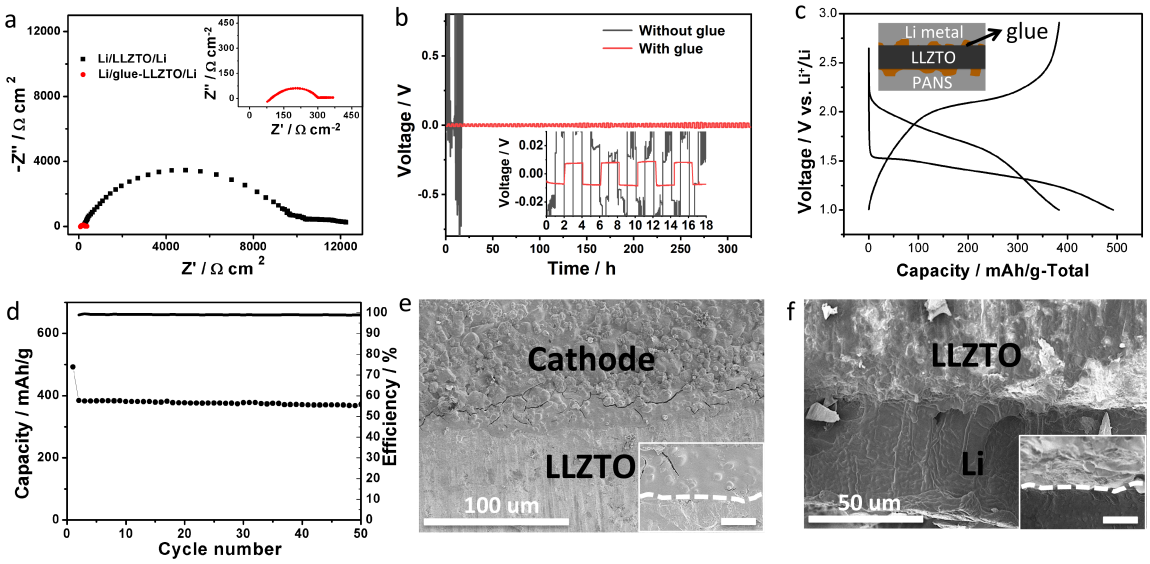


**Figure 5.** (a) EIS measurements of symmetric Li cells with/without glue. (b) Voltage profiles of the Li cells with/without glue at current densities of 0.05 mA/$cm^2$. The inset is the magnified curves. (c) 1st and 2nd charge and discharge profiles of the PANS batteries. (d) Capacity and columbic efficiency versus cycle number of the PANS batteries. The measurements were conducted at RT. (e)&(f) SEM images of the cross-section of cathode-electrolyte and Li anode-electrolyte. Scale bars in inset of figure e&f are 10 μm.

Solid-state batteries were assembled to evaluate the performance of the P@S glue modification. The Li plating and stripping behavior was firstly studied based on Li|electrolyte|Li symmetrical cells. A typical garnet LLZTO electrolyte pellets with 800 μm thick were used here. To prepare the Li|electrolyte|Li cell, a thin P@S glue coating was firstly applied to both sides of the LLZTO surface. Then two polished Li metal foils were pressed on both sides of the LLZTO pellet and the stacked Li|electrolyte|Li cell was further heated at 80 °C for 1 h under a small pressure (0.08 MPa). A control sample was made using bare LLZTO pellet without glue coating in the same way. The obviously different interfacial impedances in the symmetric cells with and without glue were shown in Figure 5(a). The total impedances of the symmetric Li|electrolyte|Li cells with and without glue coating are 308 and 10328 Ω $cm^2$, respectively. The total impedance for the LLZTO samples is 101 Ω $cm^2$, which is calculated from the EIS measurements of the Au|LLZTO|Au blocking electrode symmetric cells (Figure S14). That means the interfacial area specific resistance between Li and LLZTO decreased from 5114 Ω $cm^2$ (without glue) to 104 Ω $cm^2$ (with glue). The calculation details can be found in Supporting Information. As expected, the symmetric cell with P@S glue-coating LLZTO delivered stable plating/stripping behavior. It showed stable and flat plating and stripping curves with a small overpotential when cycled at 0.05 mA/$cm^2$, (Figure 5(b)). After cycling for 330 h, the voltage profiles were still stable, indicating stable cycling performance. In contrast, the symmetric Li cell with bare LLZTO exhibited poor cyclability with large voltage overpotential due to the large interfacial resistance between the Li metal and bare LLZTO, which has been widely observed in previous works.[29] These results clearly suggest that the P@S glue coating facilitates the $Li^+$ transport through the solid Li|electrolyte interface.

All-solid-state Li-S batteries (using PANS as cathode) with P@S glue were selected to further study the battery performance. LLZTO ceramic pellet was again used as solid

electrolyte. Similarly, the all-solid-state batteries showed decreased total resistance as compared with that of batteries without glue modification (Figure S15), indicating that the P@S glue coating also facilitates the $Li^+$ transport through the solid cathodelelectrolyte interface. Besides, the glue can easily infiltrate into the cathode and lead to a densification of the cathode after the curing process (Figure S16). Figure 5(c) show the voltage profiles of the all-solid-state batteries (see more in Figure S17). When running under 0.05 C, stable voltage profiles with low overpotential were observed. After 50 cycles, excellent capacity retention rate of 95.2% was retained, indicating a stable cycle performance of batteries (Figure 5(d)). Since there is no obvious increase in overpotential after cycling, it may be concluded that the ionic conductivity of glue coating does not change much with time. In contrast, the all-solid-state Li-S batteries without glue modification cannot be charge or discharge due to too large polarization (Figure S18). The rate perfromacne can be found in Figure S19. We tried to observe the morphological evolution of the cathode and Li anode surface after cycling. However, the strong adhesiveness makes it difficult to obtain an intact cathode layer or Li metal without residual cured glue on their surface, which in turn demonstrated the great adhesive property of the P@S glue. Alternatively, the cross section of batteries with glue coating was observed after cycling (Figure 5e&f, Figure S20&21). No obvious interfacial separate was observed for both of the cathode-electrolyte and anode-electrolyte cross section, which is consisted with the stable cycling performances.

In summary, to address the contact issue between electrode and electrolyte layers, we designed a new polymer-based electrolyte glue named P@S glue aiming to improve the interfacial contact and thus to reduce the interfacial impedance. The P@S glue is applicable to both of the cathode-electrolyte and anode-electrolyte interface. It presents great wettability with most typical electrodes and solid electrolytes, and also exhibits good adhesiveness with the substrates as well as good ionic conductivity of $1.15\times10^{-4}$ S $cm^{-1}$ (at RT) after a "pre-polymerization – post-curing" process. The all-solid-state Li-S batteries with the glue

modification show significantly reduced impedance, and exhibit stable cycling performances at room temperatures. Compared to high-density metal oxides or inorganic modification layers constructed via physical deposition methods, the lightweight yet high-strength polymer-based glue electrolyte is simple to synthesize, convenient to apply, and suitable for large-scale production. Following this strategy, the development of advanced multi-functional glues for all-solid-state LIBs in the future is promising, considering the almost unlimited possibility in polymer design and synthesis.

## ASSOCIATED CONTENT

**Supporting Information**. Experimental procedures and additional electrochemical characterization. This material is available free of charge via the Internet at http://pubs.acs.org.

## AUTHOR INFORMATION


### Corresponding Author

* L.W.C. (email: lwchen2008@sinano.ac.cn); H.W.C. (email: hwchen@hqu.edu.cn).


### Notes

† These authors contributed equally to this work.

The authors declare no competing financial interest.

## ACKNOWLEDGMENT


This work was supported by the National Natural Science Foundation of China (Grant Nos. 21703072, 21625304, 21733012). H.C. acknowledges the support from the Promotion Program for Young and Middle-aged Teacher in Science and Technology Research of

Huaqiao University and the Program for Innovative Research Team in Science and Technology in Fujian Province University. D. D. and B. Z. acknowledges the support from the Subsidized Project for Postgraduates'Innovative Fund in Scientific Research of Huaqiao University

REFERENCES

(1) Xu, K. *Chem. Rev.* **2004,** 104, (10), 4303-4417.
(2) Tarascon, J. M.; Armand, M. *Nature* **2001,** 414, (6861), 359-367.
(3) Lin, D. C.; Liu, Y. Y.; Cui, Y. *Nat. Nanotech.* **2017,** 12, (3), 194-206.
(4) Shen, Y.; Zhang, Y.; Han, S.; Wang, J.; Peng, Z.; Chen, L. *Joule* **2018,** 2, (9), 1674-1689.
(5) Li, G.; Gao, Y.; He, X.; Huang, Q.; Chen, S.; Kim, S. H.; Wang, D. *Nat. Commun.* **2017,** 8, 850.
(6) Gao, Y.; Wang, D.; Li, Y. C.; Yu, Z.; Mallouk, T. E.; Wang, D. *Angew. Chem. Int. Ed.* **2018,** 57, (41), 13608-13612.
(7) Bachman, J. C.; Muy, S.; Grimaud, A.; Chang, H. H.; Pour, N.; Lux, S. F.; Paschos, O.; Maglia, F.; Lupart, S.; Lamp, P.; Giordano, L.; Shao-Horn, Y. *Chem. Rev.* **2016,** 116, (1), 140-162.
(8) Quartarone, E.; Mustarelli, P. *Chem. Soc. Rev.* **2011,** 40, (5), 2525-2540.
(9) Ceder, G.; Ong, S. P.; Wang, Y. *Mrs Bulletin* **2018,** 43, (10), 746-751.
(10) Wu, B. B.; Wang, S. Y.; Evans, W. J.; Deng, D. Z.; Yang, J. H.; Xiao, J. *J. Mater.Chem. A* **2016,** 4, (40), 15266-15280.
(11) Manthiram, A.; Yu, X. W.; Wang, S. F. *Nat. Rev. Mater.* **2017,** 2, (4).
(12) Luo, W.; Gong, Y. H.; Zhu, Y. Z.; Fu, K. K.; Dai, J. Q.; Lacey, S. D.; Wang, C. W.; Liu, B. Y.; Han, X. G.; Mo, Y. F.; Wachsman, E. D.; Hu, L. B. *J. Am. Chem. Soc.* **2016,** 138, (37), 12258-12262.
(13) Han, X. G.; Gong, Y. H.; Fu, K.; He, X. F.; Hitz, G. T.; Dai, J. Q.; Pearse, A.; Liu, B. Y.; Wang, H.; Rublo, G.; Mo, Y. F.; Thangadurai, V.; Wachsman, E. D.; Hu, L. B. *Nat. Mater.* **2017,** 16, (5), 572.
(14) Zhou, W. D.; Wang, S. F.; Li, Y. T.; Xin, S.; Manthiram, A.; Goodenough, J. B. *J. Am. Chem. Soc.* **2016,** 138, (30), 9385-9388.
(15) Gao, H.; Xue, L.; Xin, S.; Park, K.; Goodenough, J. B. *Angew. Chem. Int. Ed.* **2017,** 56, (20), 5541-5545.
(16) Zhang, P.; Li, M.; Yang, B.; Fang, Y.; Jiang, X.; Veith, G. M.; Sun, X.-G.; Dai, S. *Adv. Mater.* **2015,** 27, (48), 8088-8094.
(17) Alarco, P. J.; Abu-Lebdeh, Y.; Abouimrane, A.; Armand, M. *Nat. Mater.* **2004,** 3, (7), 476-481.
(18) Lapique, F.; Redford, K. *Adhesion and Adhesives* **2002,** 22, (4), 337-346.
(19) Li, J. Z.; Huang, X. J.; Chen, L. Q. *J. Electrochem. Soc.* **2000,** 147, (7), 2653-2657.

(20) Hu, C.; Chen, H.; Shen, Y.; Lu, D.; Zhao, Y.; Lu, A.-H.; Wu, X.; Lu, W.; Chen, L. *Nat. Commun.* **2017,** 8, 479.
(21) Chen, H.; Wang, C.; Hu, C.; Zhang, J.; Gao, S.; Lu, W.; Chen, L. *J. Mater. Chem. A* **2015,** 3, (4), 1392-1395.
(22) Kohl, J. G.; Singer, I. L. *Prog. Org. Coat.* **1999,** 36, (1-2), 15-20.
(23) Whitfield, P. S.; Abouimrane, A.; Davidson, I. J. *Solid State Ionics* **2010,** 181, (15-16), 740-744.
(24) Umar, Y.; Morsy, M. A. *Spectrochim. Acta A* **2007,** 66, (4-5), 1133-1140.
(25) W., M. J. *J Phys. Chem.* **1926,** 30, 114.
(26) Xue, Z.; He, D.; Xie, X. *J. Mater. Chem. A* **2015,** 3, (38), 19218-19253.
(27) Diederichsen, K. M.; Buss, H. G.; McCloskey, B. D. *Macromolecules* **2017,** 50, (10), 3832-3841.
(28) Yue, L.; Ma, J.; Zhang, J.; Zhao, J.; Dong, S.; Liu, Z.; Cui, G.; Chen, L. *Energy Storage Mater.* **2016,** 5, 139-164.
(29) Shao, Y.; Wang, H.; Gong, Z.; Wang, D.; Zheng, B.; Zhu, J.; Lu, Y.; Hu, Y.-S.; Guo, X.; Li, H.; Huang, X.; Yang, Y.; Nan, C.-W.; Chen, L. *Acs Energy Lett.* **2018,** 3, (6), 1212-1218.

Insert Table of Contents Graphic and Synopsis Here. (TOC)